

Signatures of first-order phase transition in heavy-ion collisions

Ayon Mukherjee
with

Veronica Dexheimer, Tetyana Galatyuk, Ralf Rapp, Stefan Schramm, Fabian Seck, Jan Steinheimer & Joachim Stroth

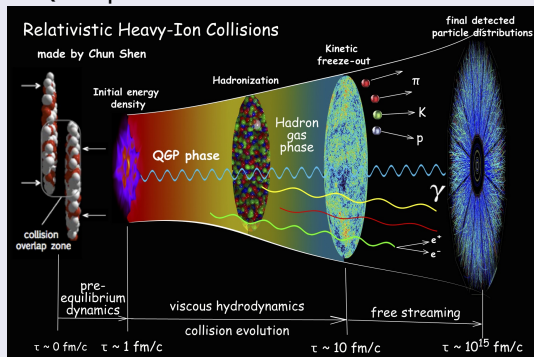
Department of Atomic Physics
Eötvös Loránd Tudományegyetem
Budapest, Hungary

December 7-11, 2020

The Background

HIC & QCD

- Stages of evolution of heavy-ion collisions
- HIC's to probe QCD phase structure



Courtesy: Chun Shen, The Ohio State University

- Use of hydrodynamics to track temporal evolution in the equilibrium stage

The Background (contd.)

Ideal Relativistic Hydrodynamics

- Macroscopic description of ideal fluid \rightarrow conserved quantities important in description of system
- Ideal fluid: a continuous system of infinitesimal volume elements, each of which are assumed to be very close to thermodynamic equilibrium
- Conservation laws: $\nabla_\mu T^{\mu\nu}_{(0)} = 0$, $\partial_\mu N^\mu_{(0)} = 0$
- Fields: ε , P , n and u^μ - corresponding to 6 degrees-of-freedom
- Equations of motion:

$$\begin{aligned} D\varepsilon + (\varepsilon + P)\theta_\mu u^\mu &= 0 \\ (\varepsilon + P)Du^\alpha + c_s^2\theta^\alpha\varepsilon &= 0 \\ Dn + n\partial_\mu u^\mu &= 0 \end{aligned}$$

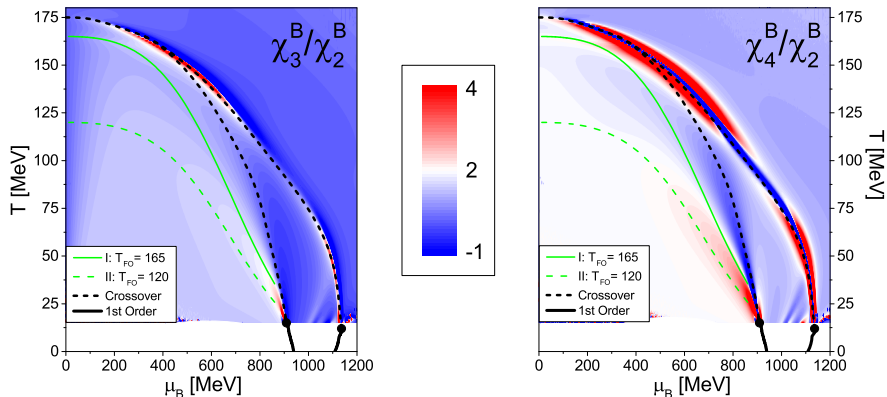
- $c_s(\varepsilon) = \sqrt{\frac{\partial P(\varepsilon)}{\partial \varepsilon}}$; EoS: $P \equiv P(n, \varepsilon)$ from thermodynamic model based on microscopic theory of strong interactions

The Thermodynamic Model I

The Quark-Hadron Chiral Parity-doublet Model ($Q\chi P$)

- Flavour SU(3) extension of a non-linear representation of the $\sigma - \omega$ model
- $\sigma \rightarrow$ order-parameter for chiral transitions, Polyakov loop $\phi \rightarrow$ order-parameter for deconfinement + excluded-volumes to remove hadrons post deconfinement
- Reproduction of reasonable values of ground-state nuclear properties
- Exploration of the effects of both the nuclear liquid-gas (LG) and the first-order chiral/deconfinement phase transitions on the behaviour of the cumulants of conserved charges, within the same effective model
- Application of the EoS i.e., $P \equiv P(n, \varepsilon)$; produced by this grand-canonical, thermodynamic analysis; to fluid-dynamic (or hydrodynamic) simulations of HIC's
- Application to neutron star matter and extraction of astrophysically viable symmetry energy, slope parameter, max. mass and radius values
- Qualitative agreement with LQCD results

The Thermodynamic Model II: Phase Diagrams

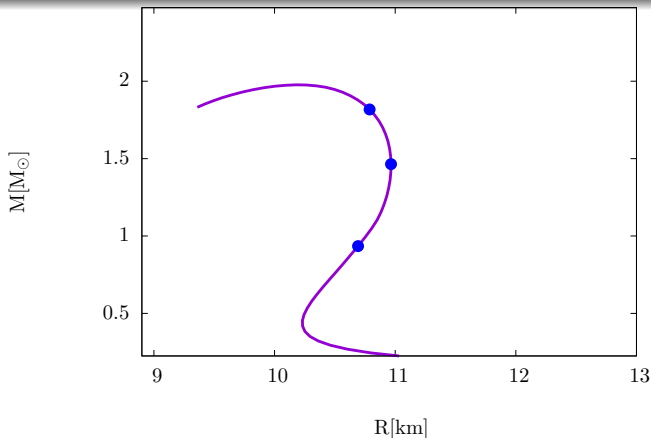


Source: AM, J. Steinheimer & S. Schramm [Phys. Rev. C 96 (2017) no.2, 025205]

The Thermodynamic Model III: Astrophysical Benchmarks

The $Q\chi P$ EoS & the TOV equations

Complete Equation of State used in the Tolman-Oppenheimer-Volkoff (TOV) equations to generate mass-radius diagram for neutron stars



Source: AM, J. Steinheimer, S. Schramm & V. Dexheimer [Astron. Astrophys. 608 (2017) A110]

The Thermodynamic Model IV

'Numbers' speak louder than words!

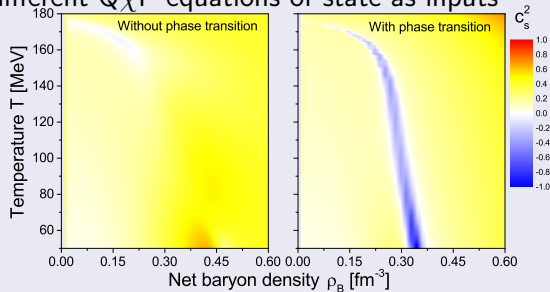
- Ground-state nuclear-matter compressibility (κ) = 267.12 MeV
- Saturation density (ρ_0) = 0.142 fm^{-3}
- Binding energy (E/A), *a.k.a.*:
Energy density per baryon (ε/ρ_B) = -16 MeV
- Symmetry energy: $S = \frac{1}{8} \left[\frac{d^2(\varepsilon/\rho_B)}{d(l_3/B)^2} \right]_{\rho_B=\rho_0} = 30.02 \text{ MeV}$
- Slope parameter: $L = 3\rho_0 \left[\frac{dS}{d\rho_B} \right]_{\rho_B=\rho_0} = 56.86 \text{ MeV}$
- Maximum star mass: $M_{\text{max}} = 1.98 M_{\odot}$
- Maximum star radius: $R_{\text{max}} = 10.25 \text{ km}$
- Canonical star mass: $M_c = 1.4 M_{\odot}$
- Canonical star radius: $R_c = 11.10 \text{ km}$

Dileptons

- Dileptons: effective probes for the early evolution of the fireball; on account of electro-weak interactions being unlikely at strong interaction timescales
- Dilepton phase-space distributions $\rightarrow T$, collectivity, emissivity of QCD medium
- The invariant mass spectrum of the dileptons is obtained from the emissivity $\epsilon = Kf^B(q_0, T)\rho_{EM}/M^2$
- Invariant mass $M = \sqrt{q_0^2 - q^2}$
- The HADES experiment (GSI/SIS18); with beam-energy scans at 1.23 AGeV using an Au+Au nuclear collision; can measure M
- Hadronic transport model, using UrQMD
- Hydro evolution, without first-order phase transition
- Hydro evolution, with first-order phase transition

Hydro simulations & the equations-of-state

- Using two different $Q\chi P$ equations of state as inputs

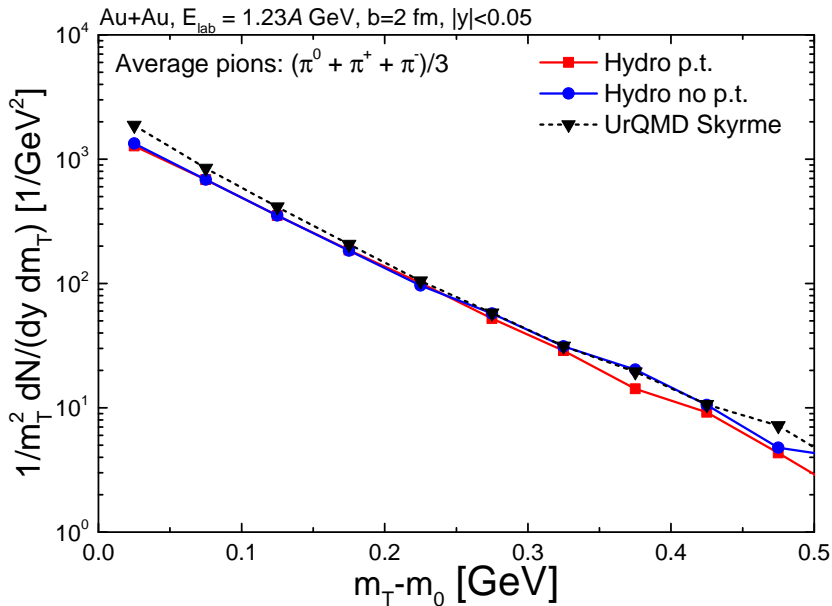


F. Seck, T. Galatyuk, A. Mukherjee, R. Rapp, J. Steinheimer, J. Stroth [arXiv:2010.04614]

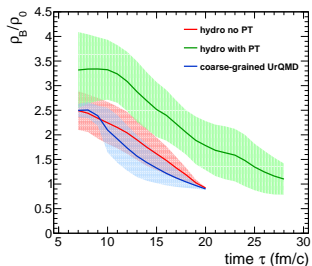
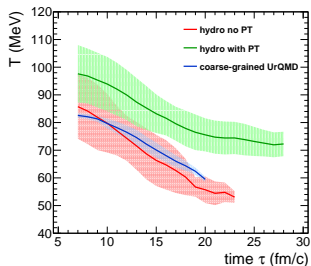
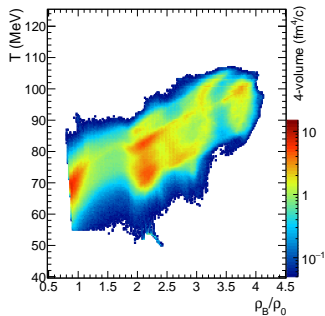
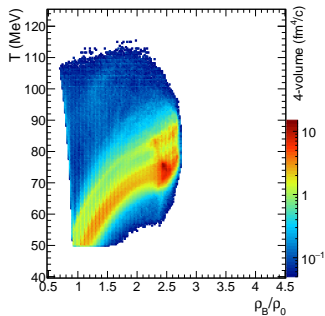
two hydrodynamic simulations are run, for three different impact parameters: 2 fm, 4 fm & 7 fm

- The resulting T and ρ_B , obtained as functions of x and t , are used to calculate the emissivity and M

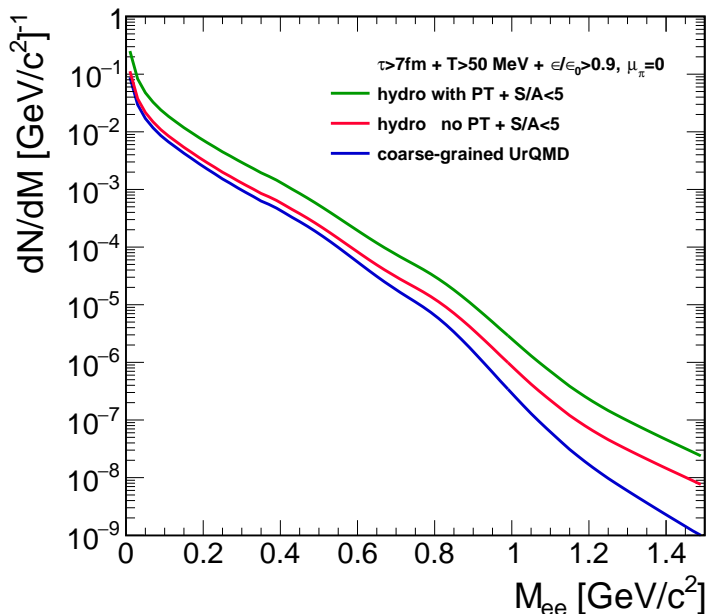
The Outcomes I: Pion m_T Spectrum



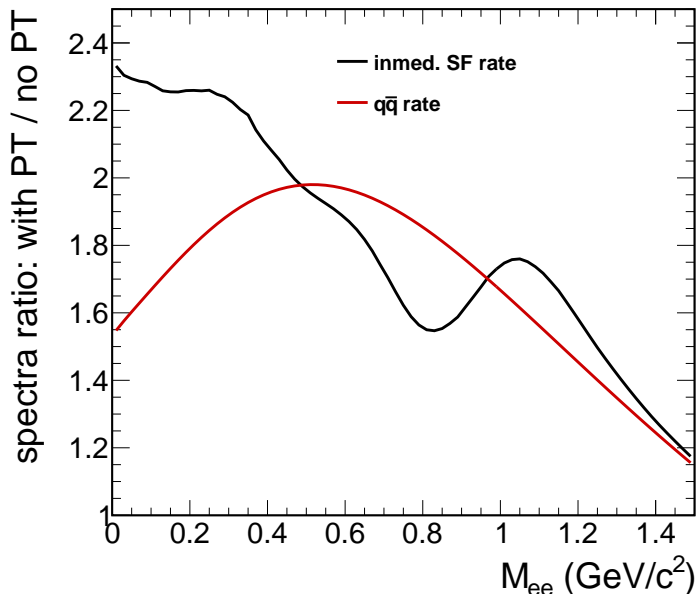
The Outcomes II: T & ρ_B



The Outcomes III: Invariant-mass Spectrum of Dileptons I



The Outcomes III: Invariant-mass Spectrum of Dileptons II



The Summary

Conclusions

- Considerable influence of LG transition on cumulant values
- Phenomenologically acceptable values for nuclear-matter compressibility, saturation density and energy density per baryon, despite inclusion of excluded-volume corrections which stiffen the EoS
- Generation of observationally vindicated values for maximum mass, canonical mass and canonical radius in neutron star family
- First-order phase transition leads to a substantial increase of the low-mass thermal dilepton yield over that from a crossover transition, by about a factor of two, as a consequence of the prolonged lifetime caused by the mixed-phase formation
- The dilepton spectrum from the crossover evolution shows good agreement with the one from coarse-grained transport
- In-medium effects on SF's lead to an additional relative enhancement at masses around 0.2 GeV in the 1st-order scenario, due to higher avg. densities in the more compressible medium with mixed phase

The Outlook

Coming soon... in journals near you

- Further quantitative investigations in comparison to existing HADES data (excitation function measurements at SIS 100 interesting!)
- Extension of the $Q\chi P$ to finite nuclei
- Effects of isospin-symmetry breaking on the model, and in turn on HIC's
- Magnetic field effects on the QCD phase diagram and fluctuations, using the $Q\chi P$
- Better agreement between $Q\chi P$ and LQCD calculations
- Tidal deformation calculations for NS's, with the $Q\chi P$ EoS
- Further exploration of the properties of ground-state nuclear-matter inside neutron stars, for different charge fractions

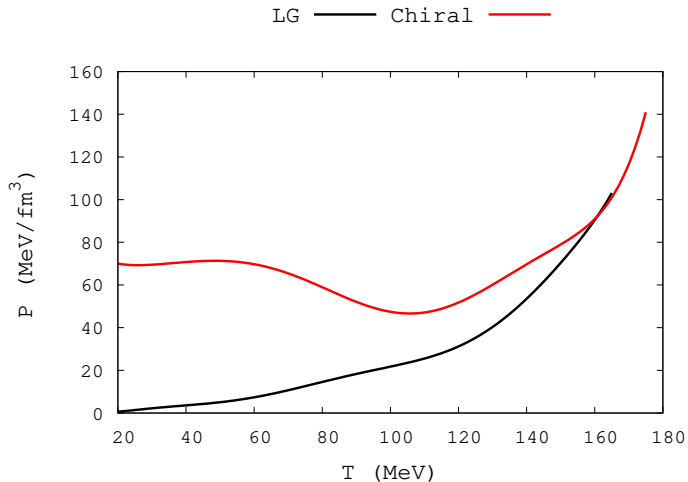
The End

Thank you for your attention!

অপ্তরে অতৃপ্তি রবে সাস্ক করি' মনে হবে
শেষ হয়ে হইল না শেষ।

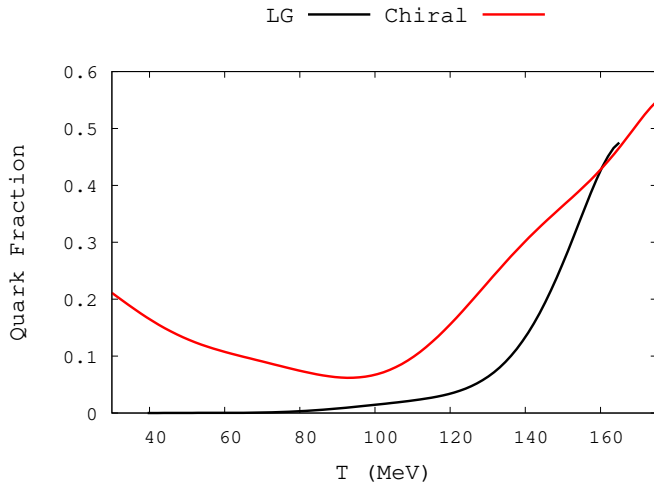
The Backup: Pressure

$$P = -\Omega = (T \ln \mathcal{Z})/V$$



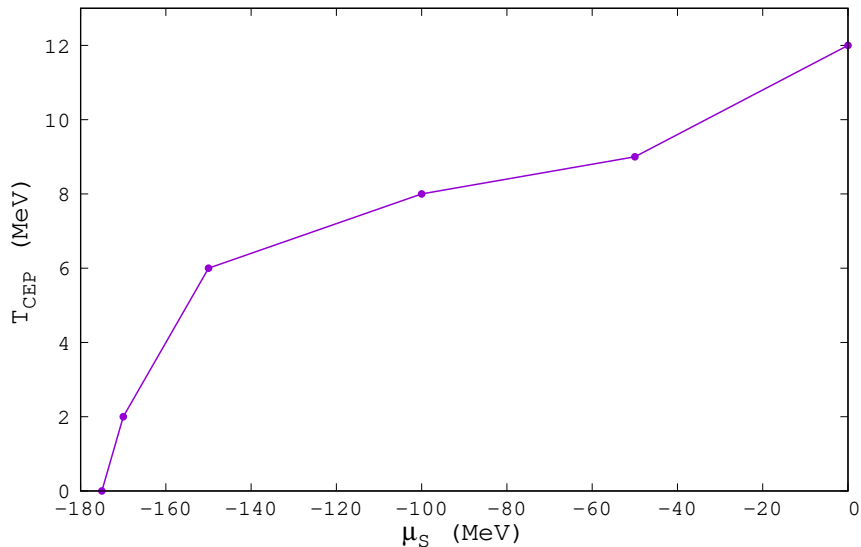
The Backup: Quark fraction

$$q_f = (\varepsilon_{\text{quark}} + \varepsilon_{\text{Polyakov}}) / (\varepsilon_{\text{baryon}} + \varepsilon_{\text{meson}} + \varepsilon_{\text{Polyakov}})$$

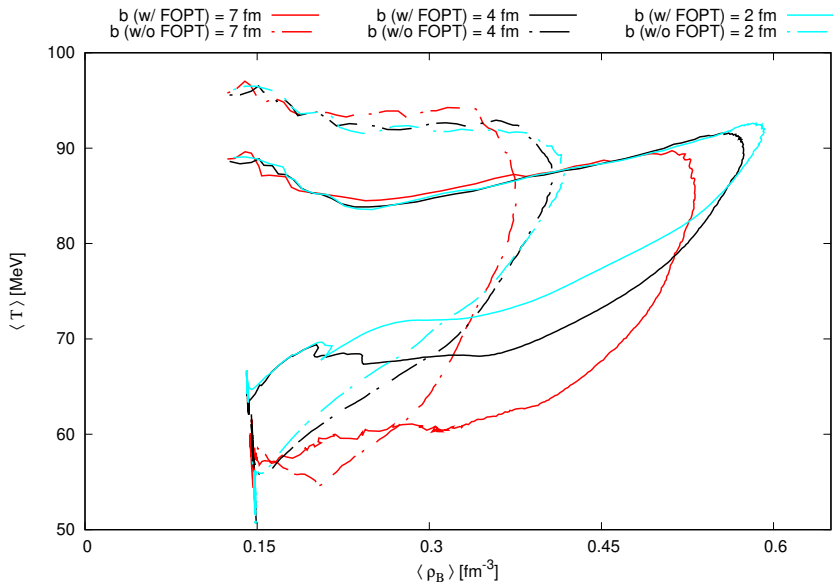


The Backup: Critical end-point

Chiral Transition



The Backup: Phase-space



The Cruc

- Lagrangian used:

$$\mathcal{L}_B = \sum_i [\bar{B}_i i \not{\partial} B_i + \bar{B}_i m_i^* B_i + (\bar{B}_i \gamma_\mu (g_{\omega i} \omega^\mu + g_{\rho i} \rho^\mu + g_{\phi i} \phi^\mu) B_i)]$$

- Effective baryon masses:

$$m_{i\pm}^* = \sqrt{[(g_{\sigma i} \sigma + g_{\zeta i} \zeta)^2 + (m_0 + n_s m_s)^2]} \pm g_{\sigma i} \sigma \pm g_{\zeta i} \zeta$$

where $\zeta = \langle \bar{s}s \rangle$ & $\sigma = \langle \bar{q}q \rangle$

- Scalar meson interaction potential:

$$V = V_0 + \frac{1}{2} k_0 l_2(\sigma, \zeta) - k_1 l_2^2(\sigma, \zeta) - k_2 l_4(\sigma, \zeta) + k_6 l_6(\sigma, \zeta)$$

The Model (contd.)

Quarks as degrees-of-freedom

- Quarks become the dominant degrees-of-freedom when QCD exhibits a smooth, crossover-like, deconfinement transition from the hadron gas, making a hadronic parity-doublet model an inadequate description of the system
- Polyakov loop Φ , which goes from 0 to 1 during deconfinement, added as order parameter for deconfinement transition to a chiral parity-doublet model:

$$\Phi = \frac{1}{3} \text{Tr} \left[\exp \left(i \int d\tau A_4 \right) \right]$$

- The thermal contribution, to the grand-canonical potential (Ω), of the quarks-to-Polyakov loop coupling:

$$\Omega_{q \text{ or } \bar{q}} = -T \sum_{i \in Q} \frac{\gamma_i}{(2\pi)^3} \int d^3k \ln \left(1 + \Phi \exp \frac{E_i^* \pm \mu_i}{T} \right)$$

The Grand Canonical Potential

- All thermodynamic quantities: energy density ε , entropy density s , and densities of the different particle species ρ_i , are derived from the grand-canonical potential.
- Effective potential $U(\Phi, \Phi^*, T)$:

$$U = -\frac{1}{2}a(T)\Phi\Phi^* + b(T) \ln [16\Phi\Phi^* + 4(\Phi^3\Phi^{*3}) - 3(\Phi\Phi^*)^2] ,$$

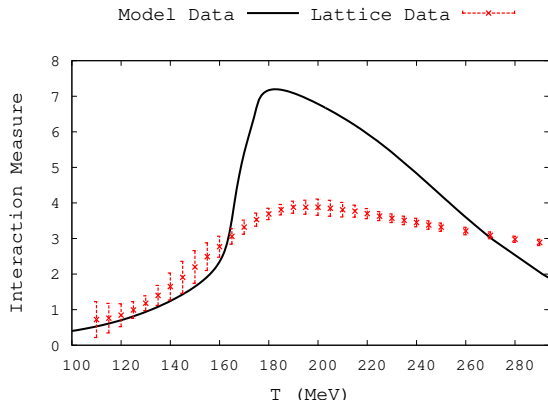
contained within the grand-canonical potential, controls the dynamics of the Polyakov loop

- Excluded volumes introduced as a way to remove hadrons following the deconfinement of quarks; modifying the effective chemical potential of the hadrons, resulting in their suppression once the quarks and gluons start contributing to the thermodynamic potential of the system

The Results I

Lattice data comparison

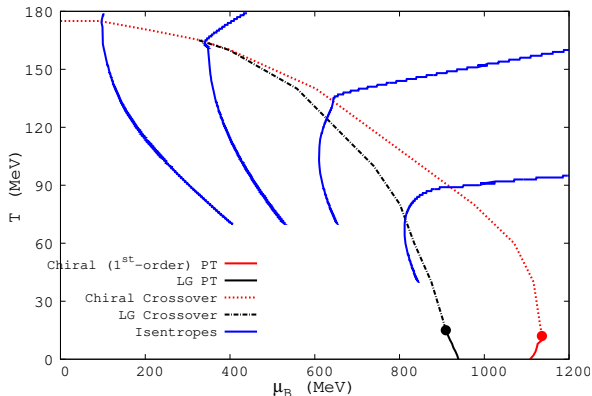
- The model parameters are constrained by actual observables at large ρ_B & low T , not by lattice results at $\mu_B = 0$
- Interaction measure, $I = (\varepsilon - 3P)/T^4$, used as means of comparison



The Results I (contd.)

The $T - \mu_B$ diagram

- PT lines defined as $(\partial\sigma/\partial\mu_B)_{\max}$, or as $(\partial\rho_B/\partial\mu_B)_{\max}$
- A double-Gaussian is fit to the derivatives with each peak assigned to a separate crossover line



The Results I (contd....)

Baryon-number susceptibilities

- Cumulants or susceptibilities (χ_n^B):

$$\frac{\chi_n^B}{T^2} = n! c_n^B(T) = \frac{\partial^n (P(T, \mu_B)/T^4)}{\partial (\mu_B/T)^n}$$

- Freeze-out curve, from fit to experimental data:

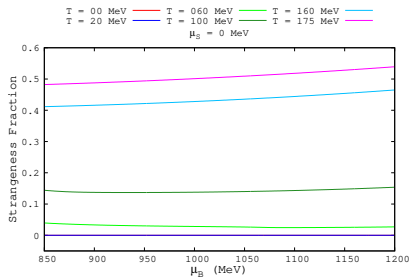
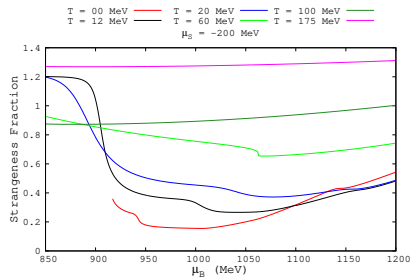
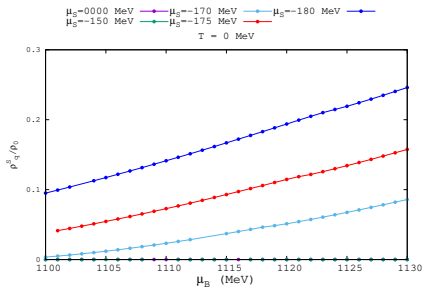
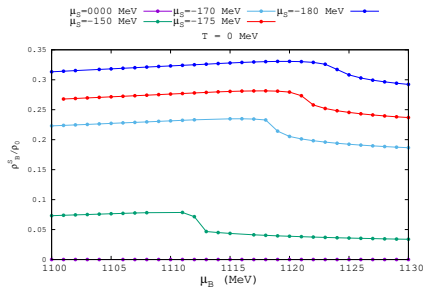
$$T \text{ (MeV)} = \frac{T_{\text{lim}}}{1 + \exp \left[2.60 - \frac{\ln(\sqrt{s_{\text{NN}}} \text{ (GeV)})}{0.45} \right]},$$

where μ_B and $\sqrt{s_{\text{NN}}}$ (the beam energy in GeV) are related as:

$$\mu_B \text{ (MeV)} = \frac{1303}{1 + 0.286\sqrt{s_{\text{NN}}} \text{ (GeV)}}$$

The Results II

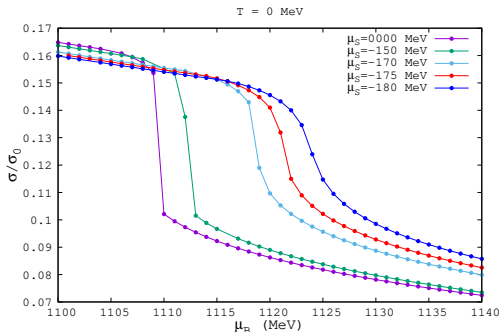
The Hyperon Rises



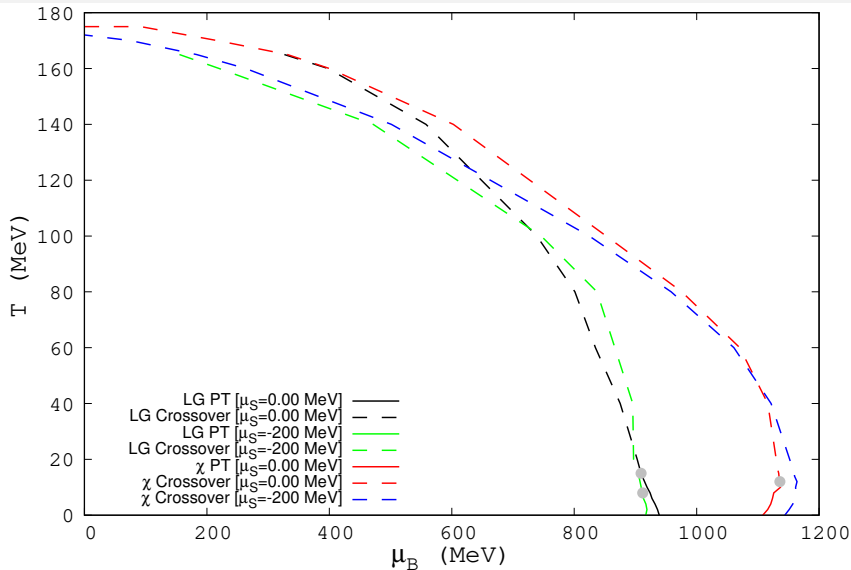
The Digression: Stranger Things

Non-zero net-strangeness chemical potential

- Theoretically, the effects of non-zero net- μ_S and net- μ_I have been well documented
- Experimentally, from fitting observed particle ratios, μ_S has been deduced to have a value of $\sim 25\% - 30\%$ of μ_B , while μ_I remains small, at around $2\% - 5\%$ of μ_B

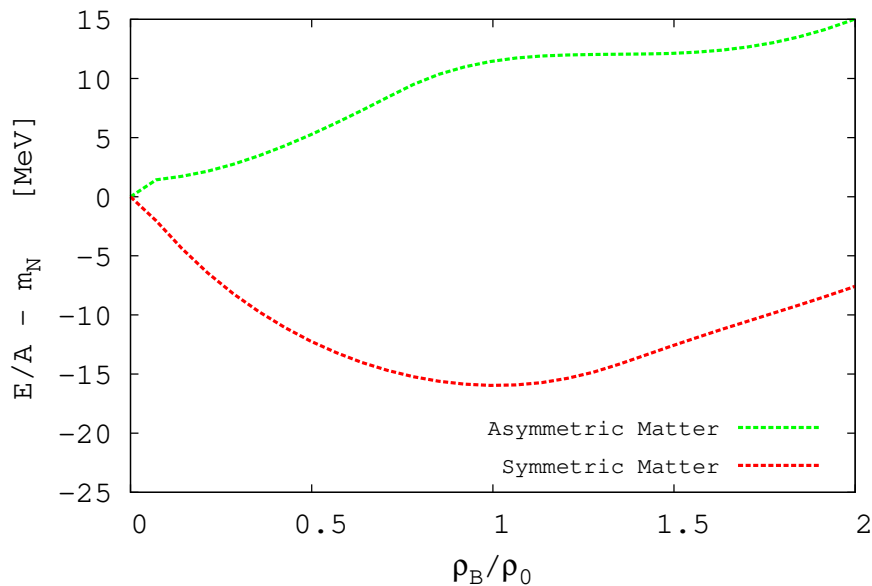


The Outcomes II: The Modified Phase Boundary



Source: AM, A. Bhattacharyya & S. Schramm [arXiv:1807.11319]

The Outcomes I (contd.): Binding & Symmetry Energies



The Outcomes (contd...): Compactness

